JOURNAL OF MATERIALS SCIENCE 18 (1983) 153–160

Mechanical properties of ductile Fe–Ni–Zr and Fe–Ni–Zr (Nb or Ta) amorphous alloys containing fine crystalline particles

A. INOUE,* H. TOMIOKA,† T. MASUMOTO
The Research Institute for Iron, Steel and Other Metals, Tohoku University, Sendai 980, Japan

Melt-quenched $Fe_{60-80}Ni_{10-30}Zr_{10}$ and $Fe_{70}Ni_{20}Zr_{10-x}$(Nb or Ta)$_x$ ($x \lesssim 2$ at %) alloy ribbons with the duplex structure consisting of amorphous and bcc phases were found to exhibit hardness and tensile strengths higher than those of the totally amorphous alloys. The volume fraction of the bcc phase was intentionally allowed to alter in the range 0% to 60% by changing the composition and sample thickness. The bcc phase has an average particle size of 75 nm for the Fe–Ni–Zr alloys and 50 nm for the Fe–Ni–Zr–Nb alloys, and the lattice parameter is much larger than that of pure α-Fe because of the dissolution of large amounts of zirconium, niobium and/or tantalum. The hardness and tensile strength of the duplex alloys increase with amount of bcc phase and reach about 880 DPN and 2580 MPa, which are higher by about 20% to 30% than those of the amorphous single state, at an appropriate volume fraction of bcc phase. As the volume fraction of the bcc phase increases further, the duplex alloys become brittle and the tensile strength decreases significantly. The enhancement of strength was considered to be due to the suppression of shear slip caused by fine bcc particles dispersed uniformly in the amorphous matrix. It was thus demonstrated that an optimum control of melt-quenched structure results in the formation of ductile Fe-based amorphous alloys containing fine crystalline particles.

1. Introduction

It is well known that an amorphous alloy possesses high strength combined with rather good ductility. However, almost all the iron-based amorphous alloys become rapidly brittle on annealing at temperatures much lower than crystallization temperature [1] as well as upon crystallization and such a catastrophic loss of ductility prevents practical applications as an engineering material. The appearance of iron-based amorphous alloys in which the ductile nature remains almost unchanged even by introducing crystalline phases has been fervently desired from the engineering point of view. Recently, it has been found that melt-quenched Fe–Ni–Zr alloys are so ductile that no cracks are observed even after a 180° bend test in a duplex state containing fine crystalline particles in an amorphous matrix as well as in an amorphous single state. It is also noticeable that the duplex alloys exhibit tensile strengths and hardness higher than those of the amorphous single phase. The aim of this paper is to present the conditions in which the amorphous alloys containing numerous fine crystalline particles form and the mechanical properties of the duplex alloys.

2. Experimental methods

Master alloys of Fe–Zr, Fe–Ni–Zr, Fe–Co–Zr, Fe–Cr–Zr and Fe–Ni–Zr–X (X = Ti, V, Nb,

*Present address: Bell Laboratories, Murray Hill, New Jersey 07974, USA.
†Present address: Unitika Research Center, Unitika Ltd, Uji 611, Japan.

0022–2461/83/010153–08$03.46/0

Ta, Cr, Mo, W, Al or Si) systems were prealloyed using high-purity metals under argon atmosphere in an arc furnace. The ingots were repeatedly turned over and remelted to ensure homogeneity of composition. Each ingot was then used to produce rapidly quenched ribbons from the melt by chill block melt-spinning in air. Typically, the amount of alloys melted in one run was about 1 g and the rotation speed of the steel roller (20 cm diameter) was controlled in the range 2000 to 6500 rpm in order to change the resultant sample thickness. The ribbons were subjected to bend ductility testing and samples able to bend through 180° were designated as being ductile. The as-quenched phase was examined by conventional X-ray diffraction and transmission electron microscopy techniques. The transmission electron microscope samples were electrolytically thinned in a solution of 90 parts ethyl alcohol and 10 parts perchloric acid, immersed in ice water. The crystallization temperature (T_x) and the heat of crystallization (ΔH) were measured using differential scanning calorimetry (Perkin Elmer DSC II) at a heat rate of 40 K min^{-1}. The heat of crystallization of $Fe_{60-90}Ni_{0-30}Zr_{8-10}Nb_{0-2}$ amorphous alloys is roughly independent of composition, and hence the crystalline fraction (V_f) of the specimens was determined from the ratio of the amount of heat released on being heated from room temperature to 900 K to the amount of heat evolved from a totally amorphous specimen on crystallization, using the following equation.

$$V_f = \frac{\Delta H_{T,Am} - \Delta H_{T,PAm}}{\Delta H_{T,Am}}$$

Here, $\Delta H_{T,Am}$ is the total enthalpy released upon crystallization of a totally amorphous sample and $\Delta H_{T,PAm}$ is the total enthalpy released upon crystallization of a partially amorphous sample. Hardness and strength of the specimens were measured by a Vickers microhardness tester with a 100 g load and an Instron-type tensile testing machine at a strain rate of 1.7×10^{-4} sec^{-1}, respectively. Eight to ten symmetrical indentations and eight tensile test data were used to determine an average microhardness value or tensile strength. Tensile specimens were cut from as-quenched ribbon into strips having a gauge dimension of 10 mm long. Subsquent to tensile testing, the cross-sectional area at the fracture site of each specimen was measured using optical microscopy in order to minimize error in the estimation of the tensile strength. Fracture surfaces were examined in the scanning electron microscope (SEM) to determine the effect of crystalline particle dispersion on the fracture surface morphology and the mode of fracture under uniaxial tension.

3. Results

3.1. Melt-quenched structure

The change in the melt-quenched structure of $Fe_{70}Ni_{20}Zr_{10}$ alloy is shown in Fig. 1 as a function of rotation speed of the roller. With decreasing rotation speed, the structure changes from homogeneously amorphous phase to duplex phases consisting of fine crystalline particles embedded in an amorphous matrix. The corresponding diffraction patterns shown in Fig. 1d and f clearly indicate that the crystalline particles have a bcc structure with a lattice parameter of $a \simeq 0.2910$ nm which corresponds to ferrite phase containing rather large amounts of zirconium and/or nickel. Hence, its composition appears to be fairly close to the nominal composition of the alloy. The bcc particles precipitate very uniformly and have an elliptical or a globular shape with a diameter as small as about 75 nm. Furthermore, one can see in Fig. 1c and e that the interfaces between bcc and amorphous phases are not perfectly spherical but develop outgrowths or cusps. The particle size appears to increase with decreasing rotation speed, but the degree of change is very slight. It is therefore inferred that the mechanical properties of the duplex alloys depend strongly on the amount of precipitation of the bcc particles.

Surprisingly, the duplex alloys consisting of bcc and amorphous phases shown in Fig. 1c exhibit a highly ductile nature and are able to sustain a 180° bend. As an example, the deformation structure of a $Fe_{70}Ni_{20}Zr_{10}$ duplex alloy subjected to a 180° bend is shown in Fig. 2. While numerous deformation markings can be seen near the bent edge, no cracks are observed, in good agreement with the deformation structure of homogeneously amorphous alloys. The similar duplex structures consisting of amorphous and bcc phases were also observed in melt-quenched $Fe_{90-x}Zr_x$, $Fe_{60-80}Cr_{10-30}Zr_{10}$ and $Fe_{60-80}Co_{10-30}Zr_{10}$ alloys. However, the duplex phases in these alloys are brittle and fracture occurs during the bend test, indicating that the addition of nickel

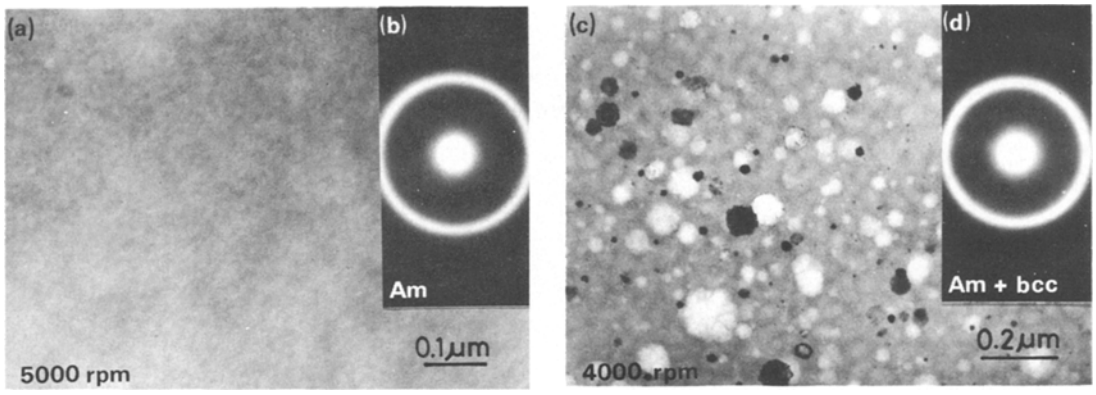

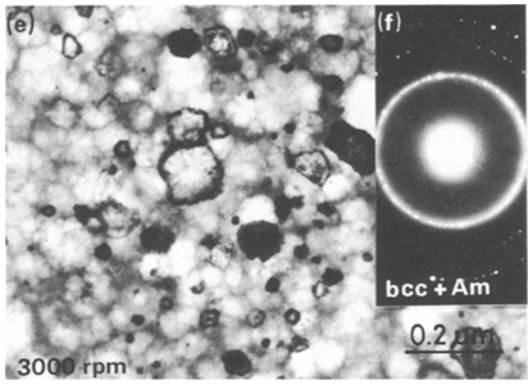

Figure 1 Change in the microstructure of melt-quenched $Fe_{70}Ni_{20}Zr_{10}$ alloys with rotation speed of roller.

is essential for the formation of the duplex phase having a highly ductile nature.

3.2. Thermal stability

Fig. 3 shows the DSC curves for $Fe_{70}Ni_{20}Zr_{10}$ alloy having an amorphous single phase and a duplex structure. Considering the result that the weight of the measured sample is almost completely the same, it is concluded that the crystallization temperature (T_x) is lower and the heat of crystallization (ΔH) is smaller for the duplex structure than for the amorphous single phase. In addition, one can see that the transition of amorphous to crystalline phases occurs over a wider temperature range for the duplex alloys compared with the amorphous single phase. This suggests that a nucleation of crystalline phase (bcc phase) occurs preferentially on the interface between amorphous and bcc phases and hence the temperature at which the bcc phase begins to appear becomes lower compared with the amorphous single phase.

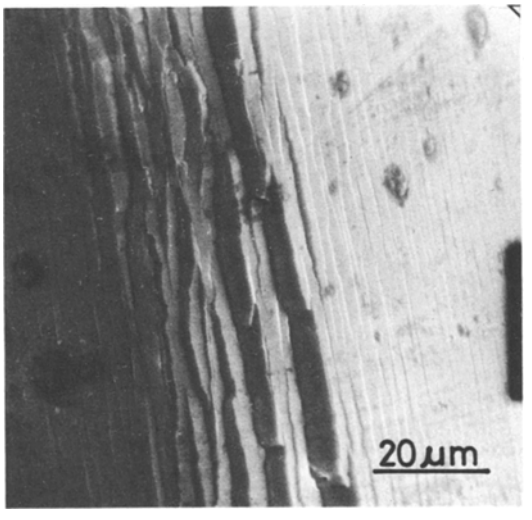

Figure 2 Scanning electron micrograph showing deformation markings on the bend surface of a duplex $Fe_{70}Ni_{20}Zr_{10}$ alloy.

3.3. Mechanical properties

The mechanical properties of the $Fe_{80}Ni_{10}Zr_{10}$ and $Fe_{70}Ni_{20}Zr_{10}$ alloys were measured in order to find a material with high strength as well as good ductility in the duplex state. Vickers hardness (H_v) and tensile fracture strength (σ_f) are shown as a function of volume fraction (V_f) of bcc phase in Fig. 4. H_v and σ_f in an amorphous state are about 600 DPN and 1850 MPa for $Fe_{80}Ni_{10}Zr_{10}$ alloy and about 550 DPN and 1550 MPa for $Fe_{70}Ni_{20}Zr_{10}$ alloy, but these values increase significantly by introducing fine bcc particles, reach about 650 DPN and 2350 MPa for $Fe_{80}Ni_{10}Zr_{10}$ and about 680 DPN and 1875 MPa for $Fe_{70}Ni_{20}Zr_{10}$, and decrease significantly with further increasing volume fraction of bcc phase. Thus, it is noticeable that the duplex alloys containing an appropriate amount of bcc phase in the amorphous matrix exhibit hardness and strengths higher than those of the amorphous

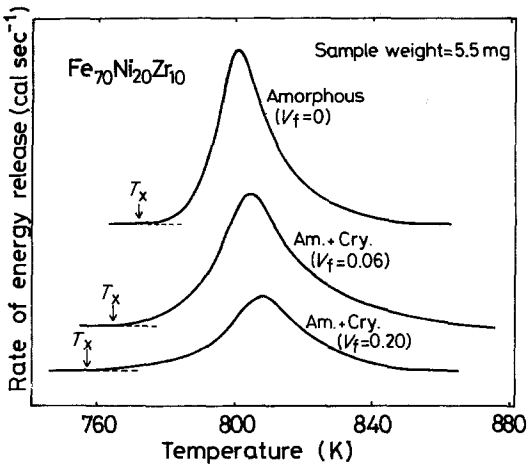

Figure 3 Differential scanning calorimetry curves of amorphous and duplex $Fe_{70}Ni_{20}Zr_{10}$ alloys.

alloys, despite the fact that the strength of the bcc phase is considered to be much lower than that of the amorphous phase. Fig. 4 also shows that the replacement of iron by nickel results in a decrease in hardness and tensile strength.

3.4. Improvement of mechanical properties by additional elements

In order to enhance the strength of the duplex phase without detriment to good bend ductility, the effect of additional elements on the micro-

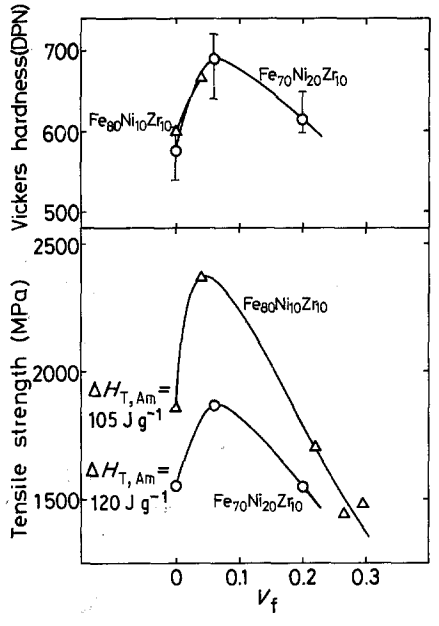

Figure 4 Changes in the Vickers hardness (H_v) and tensile fracture strength (σ_f) of melt-quenched $Fe_{80}Ni_{10}Zr_{10}$ and $Fe_{70}Ni_{20}Zr_{10}$ alloys with volume fraction of bcc particles.

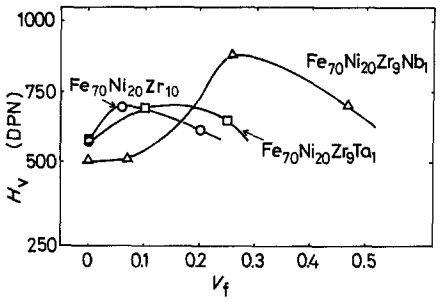

Figure 5 Change in the Vickers hardness (H_v) of melt-quenched $Fe_{70}Ni_{20}Zr_9Nb_1$ and $Fe_{70}Ni_{20}Zr_9Ta_1$ alloys with volume fraction of bcc particles. The data of $Fe_{70}Ni_{20}Zr_{10}$ alloy are also shown for comparison.

structure and mechanical properties of the duplex $Fe_{70}Ni_{20}Zr_{10}$ alloy was examined by replacing zirconium with solute elements such as titanium, vanadium, niobium, tantalum, chromium, molybdenum, tungsten, aluminium and silicon. As a result, the replacement of zirconium only by niobium or tantalum was found to be effective for improvement of mechanical properties as shown in Figs 5 and 6. However, the manner in which the values of H_v and σ_f change with the amount of bcc particles is significantly different in both the $Fe_{70}Ni_{20}Zr_9Nb_1$ and $Fe_{70}Ni_{20}Zr_9Ta_1$ alloys. The latter alloy exhibits the highest values of H_v and σ_f around $V_f \simeq 0.1$ and decreases significantly with increasing volume fraction of bcc phase, similar to the tendency for $Fe_{70}Ni_{20}Zr_{10}$ alloy. On the other hand, H_v and σ_f of $Fe_{70}Ni_{20}Zr_9Nb_1$ alloy gradually increase with the amount of bcc phase, reach maximum values of about 880 DPN and 2500 MPa, respectively, in the vicinity of $V_f \simeq 0.3$, and decrease signifi-

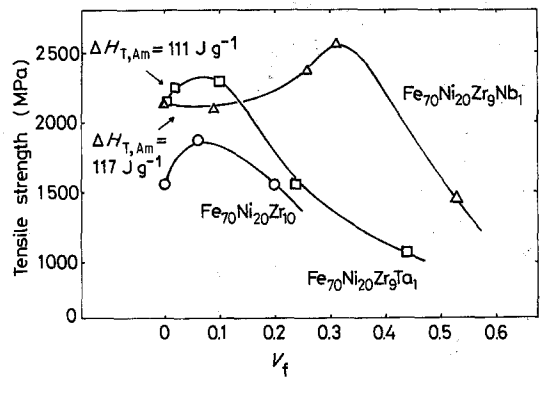

Figure 6 Change in the tensile fracture strength (σ_f) of melt-quenched $Fe_{70}Ni_{20}Zr_9Nb_1$ and $Fe_{70}Ni_{20}Zr_9Ta_1$ alloys with volume fraction of bcc particles. The data of $Fe_{70}Ni_{20}Zr_{10}$ alloy are also shown for comparison.

cantly with further increase in the amount of bcc phase. Although the reason why the niobium-containing alloy exhibits the highest values in the duplex state, containing bcc phase in amounts as large as ~ 30%, is not clear, it may be closely related to the observed result that the bcc phase in the $Fe_{70}Ni_{20}Zr_9Nb_1$ alloy has a considerably smaller particle size (≃ 50 nm) compared with the other duplex alloys, as shown in Fig. 7. One can also see that the replacement of zirconium by niobium or tantalum results in a remarkable extension of the formation range of the ductile duplex alloys. However, the amount of replacement is limited to less than about 2 at% for niobium and about 1 at% for tantalum. The replacement of zirconium by the other elements of vanadium, chromium, molybdenum or tungsten causes an enhancement of brittleness and ductile duplex alloys were not fabricated in the present study. In any event, it is concluded that the addition of a small amount of niobium or tantalum is very effective for the improvement of tensile strength and good bend ductility in the duplex state.

Typical engineering stress–elongation curves of the amorphous and duplex $Fe_{70}Ni_{20}Zr_9Nb_1$ alloys are presented in Fig. 8. The amorphous ($V_f = 0$) and duplex ($V_f = 0.31$) alloys exhibit a linear stress–elongation curve with only a small deviation from linearity noted, beginning at a stress of $\simeq 0.8\sigma_f$ and the total elongation recorded on the test chart, including elastic and plastic elongation, is about 2.5% to 3.0%. On the other hand, the duplex alloy ($V_f = 0.53$) containing a larger amount of bcc phase exhibits a completely linear stress–elongation curve with a total elongation of only 1.5% to 2.0% because of the increasing brittleness of the material. As seen in Fig. 8, the

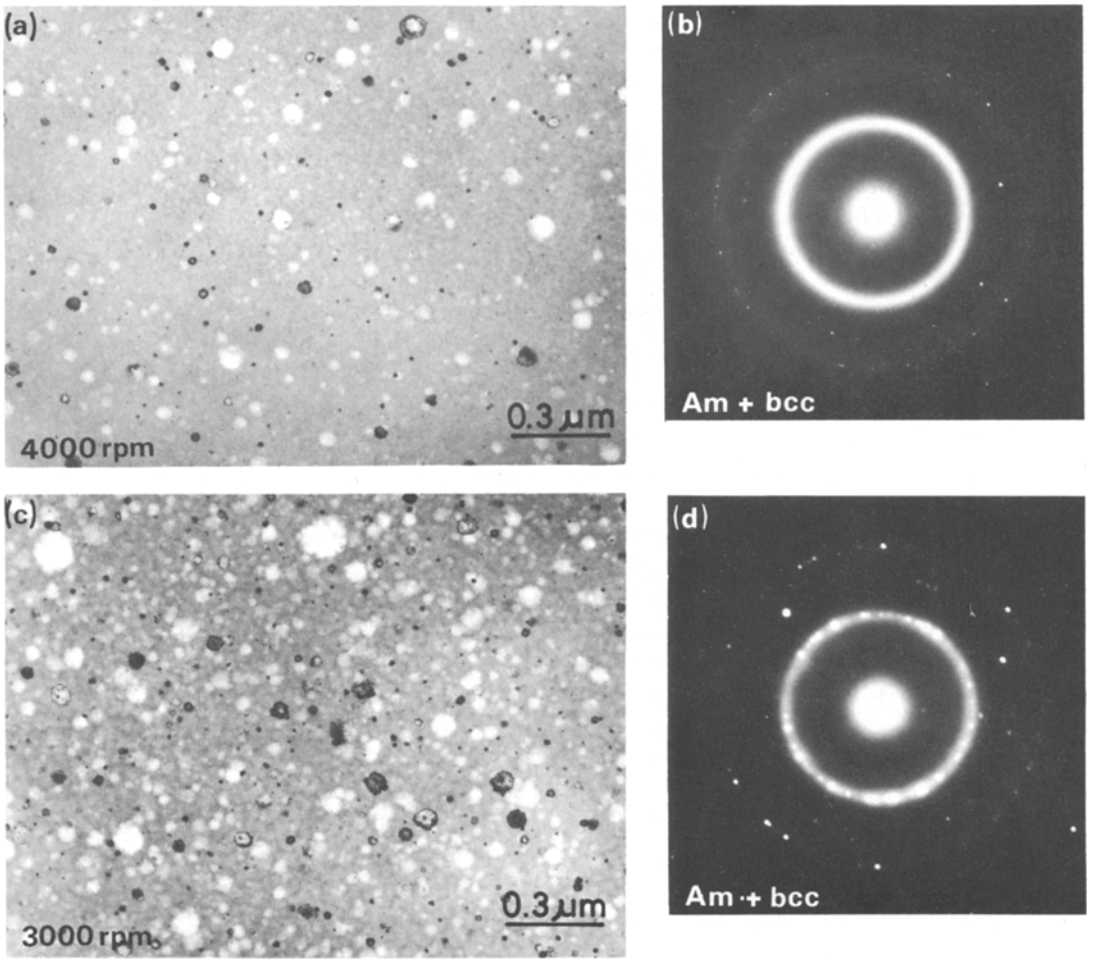

Figure 7 Transmission electron micrographs and selected-area diffraction patterns showing the duplex structure consisting of amorphous and bcc phases in melt-quenched $Fe_{70}Ni_{20}Zr_9Nb_1$ alloy.

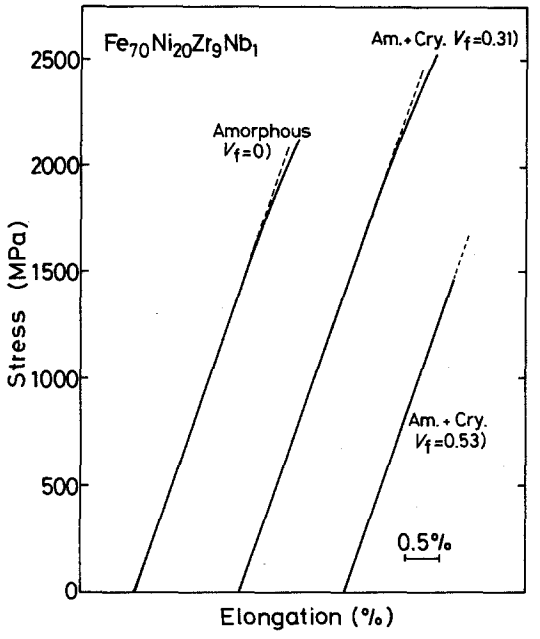

Figure 8 Change in the uniaxial tensile stress–elongation curves of melt-quenched $Fe_{70}Ni_{20}Zr_9Nb_1$ alloy with volume fraction of bcc particles.

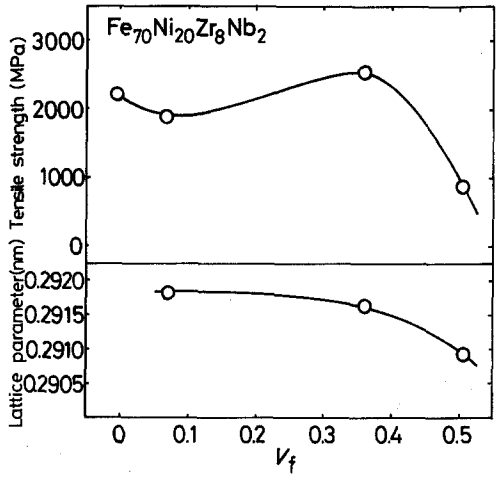

Figure 9 Change in the lattice parameter of melt-quenched $Fe_{70}Ni_{20}Zr_8Nb_2$ alloy with volume fraction of bcc particles.

enhancement of the σ_f is not due to the increase in plastic elongation, but due mainly to the increase of the proportional limit. Considering the result that the main reason for the deviation from the proportional line is due to the slipping on shear plane, the increase in σ_f appears to be due to the increasing resistance to shear deformation of the amorphous phase caused by a small V_f of fine bcc particles. No systematic change in the gradient of stress–elongation curve, corresponding to the Young's modulus, with increasing V_f was detected from the test chart.

The change in the lattice parameter of bcc particles as a function of V_f was examined for the duplex $Fe_{70}Ni_{20}Zr_8Nb_2$ alloys (Fig. 9). The lattice parameter is 0.2918 nm at $V_f = 0.06$, remains almost unchanged up to about $V_f \simeq 0.4$ and significantly decreases with further increase in V_f. These values are considerably larger than that (0.2866 nm) [2] for pure α-iron, indicating that the bcc particles dissolved large amounts of zirconium and/or niobium. The equilibrium phase diagrams of Fe–Zr and Fe–Nb systems [3] show that α-iron hardly dissolves zirconium or niobium at room temperature. Hence, it is concluded that the bcc phase in the duplex alloys is a supersaturated solid solution containing zirconium and/or niobium more than the equilibrium solubility limit. The reason for the rapid decrease in lattice parameter in the region of $V_f > 0.4$ is due to the decrease in the amount of zirconium and/or niobium in the bcc phase through the ease of rearrangement among the constituent elements by the lowering of the cooling rate. The above results suggest that the lowering of σ_f in the region of $V_f > 0.4$ is due to the decrease in volume fraction of the amorphous phase exhibiting high strength and due to the lowering of strength of the bcc particles themselves by decrease in the zirconium and/or niobium content in the particles.

3.5. Fracture morphology

The tensile fracture appearance of the duplex $Fe_{70}Ni_{20}Zr_{10}$ ($V_f = 0.06$) is shown in Fig. 10. Tensile fracture occurs on a shear plane at 45° to 50° to the thickness direction and the morphology of the fracture surface is composed of two zones. One is a relatively featureless zone (A) produced by shear slip, and the other (B) is a vein pattern produced by the rupture of the cross-section remaining after the initial shear. Thus, the features of the fracture surface for the partially amorphous alloy are very similar to that for totally amorphous alloys [4]. In particular, it should be noted that a significant fraction of the fracture surface is occupied by the featureless zone which occurred by the shear displacement experienced prior to failure. This indicates that the uniform dispersion of fine bcc particles in an amorphous matrix does not cause a significant lowering of ductility. The formation of a large number of voids and cavities

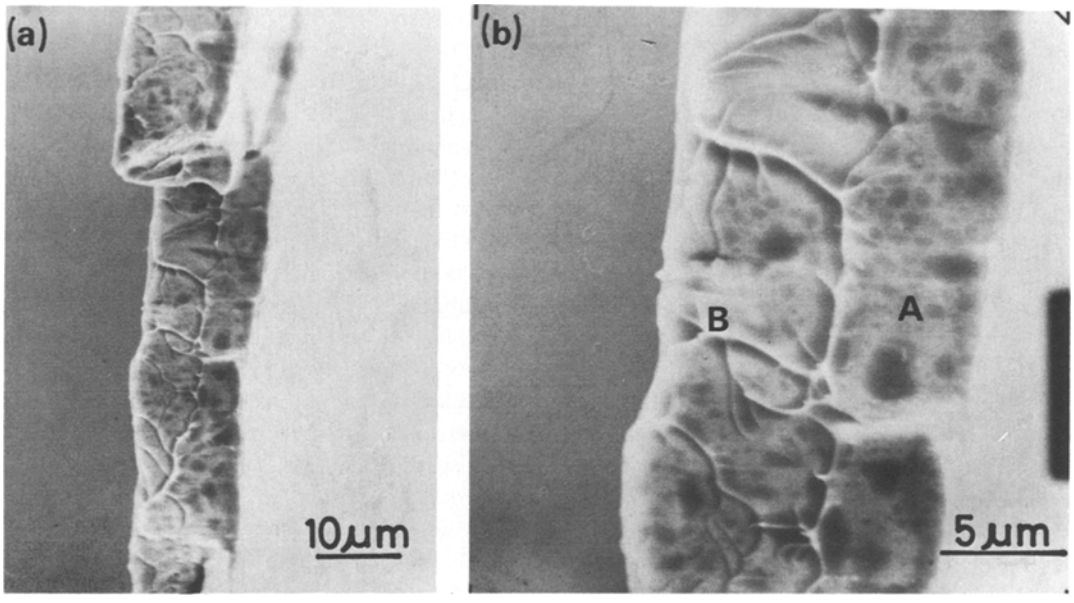

Figure 10 Scanning electron micrographs showing the tensile fracture appearance of a duplex $Fe_{70}Ni_{20}Zr_{10}$ alloy.

on the fracture surface of the duplex alloy, can also be seen resembling the dimpled rupture morphology observed in the ductile fracture of crystalline materials. This result suggests that the existence of second-phase particles exerts an influence on the fracture characteristics as sites for cavity nucleation which grow and coalesce to cause failure. However, judging from the result that the features of the fracture appearance are very similar for the partially and the totally amorphous alloys, it is pointed out that such an influence is very slight and the existence of a small volume fraction of fine bcc particles does not cause a drastic change in fracture morphology of amorphous alloys.

4. Discussion

As described in a previous section, H_v and σ_f of Fe–Ni–Zr and Fe–Ni–Zr– (Nb or Ta) alloys are higher by about 20% to 30% for the duplex state consisting of amorphous and bcc phases than for the amorphous single state. In order to clarify the mechanism for the increases in hardness and tensile strength of the duplex alloys, mechanical strength data were analysed based on the so-called "mixture rule". H_v and σ_f of the bcc phase itself are reasonably considered to be considerably lower than those of the amorphous phase, even though the bcc particles dissolve large amounts of zirconium, niobium and/or tantalum which are much more than the equilibrium solubility limit. Therefore, the enhancement of H_v and σ_f by the introduction of fine bcc particles cannot be explained by the "mixture rule".

This enhancement may be considered to be closely related to the unique deformation and fracture behaviour of amorphous alloys. That is, the plastic deformation and fracture of an amorphous ribbon in the uniaxial tensile test occur through the process of a slight shear slip followed by a final rupture. Consequently, the suppression of the shear slip prior to fracture is considered to result in an increase in σ_f. Although the strength of the bcc phase is lower than that of the amorphous phase, there is a high possibility that numerous fine bcc particles dispersed in the amorphous matrix may act as barriers against the shear displacement because of the strain field around individual particles. This inference also receives support from the result (Fig. 8) that the increase in σ_f is due to the increase in the proportional limit in the stress–elongation curve.

Group IV, V and VI transition metals (Ti, V, Nb, Ta, Cr, Mo, W) of the Periodic Table were added in order to enhance the mechanical strengths of the duplex alloys. As a result, only niobium and tantalum elements were found to be useful for the enhancement of strength without detriment to good bend ductility. The effectiveness of these elements appears to be closely related to the following characteristics: (1) considering the result [5] that Fe–Nb and Fe–Ta alloys containing only

2 at% B form an amorphous single phase, the replacement of zirconium by niobium or tantalum does not result in a remarkable lowering in the amorphous phase-forming ability; (2) the dissolution of niobium or tantalum suppresses the grain growth of the bcc particles and results in the uniform precipitation of particles having smaller sizes. Other solute elements also have a similar resisting effect against grain growth, but the amorphous phase-forming ability is remarkably lowered by the replacement of zirconium with the other elements. Hence duplex alloys in which the major phase consists of larger sized bcc particles are formed, resulting in an increased brittleness of the material.

5. Conclusion

The as-quenched structures and mechanical properties of $Fe_{90-x}Ni_xZr_{10}$ and $Fe_{70}Ni_{20}Zr_{10-x}X_x$ (X = Ti, V, Nb, Ta, Cr, Mo, W, Al, Si) alloys rapidly quenched from the melt were examined by transmission electron microscopy, X-ray diffraction, Vickers hardness measurement and tensile tests. The results obtained can be summarized as follows.

(1) Ductile duplex alloys containing bcc particles in the amorphous matrix were produced in the composition ranges 10 to 30 at% Ni for the Fe–Ni–Zr system and less than 2 at% Nb or 1 at% Ta for the Fe–Ni–Zr–X system. The volume fraction of the bcc particles was intentionally allowed to alter by 0 to 60% by changing the compositions and the sample thickness. The bcc particles had an average diameter of 50 to 75 nm and the lattice parameter was considerably larger than that of pure α-iron because of the dissolution of large amounts of zirconium, niobium and/or tantalum.

(2) The hardness (H_v) and tensile fracture strength (σ_f) of the duplex alloys increased with the amount of bcc phase without detriment to good bend ductility, and reached the highest values of about 880 DPN and 2580 MPa, which were higher by about 20% to 30% than those of the homogeneously amorphous alloys, at an appropriate volume fraction of the bcc phase. As the volume fraction increased further, the duplex alloys eventually embrittled and σ_f decreased significantly. The increases in H_v and σ_f were considered to be due to the suppression of shear displacement caused by fine bcc particles dispersed uniformly in the amorphous matrix.

In conclusion, it may be stated that the formation of the ductile duplex iron-based alloys consisting of amorphous and crystalline phases is very attractive from the fundamental and engineering points of view.

References

1. H. S. CHEN and D. E. POLK, *J. Non-Cryst. Solids* **15** (1974) 174.
2. W. B. PEARSON, "A Handbook of Lattice Spacings and Structures of Metals and Alloys" (Pergamon Press, London, 1958) p. 125.
3. C. J. SMITHELLS, "Metals Reference Book", 5th edn (Butterworths, London, 1976) pp. 607, 623.
4. H. J. LEAMY, H. S. CHEN and T. T. WANG, *Met. Trans.* **3** (1972) 699.
5. A. INOUE, K. KOBAYASHI, M. NOSE and T. MASUMOTO, *J. Phys. Colloque-8* **41** (1980) 831.

Received 24 May
and accepted 14 June 1982